



# The Open Chemical Engineering Journal

Content list available at: <https://openchemicalengineeringjournal.com>



## RESEARCH ARTICLE

### Computational Simulation of Atherosclerosis Progression Associated with Blood Pressure in a 2-D Idealized Human Carotid Artery Model

Edith E. Alagbe<sup>1\*</sup>, Temiloluwa E. Amoo<sup>1</sup>, Augustine O. Ayeni<sup>1</sup>, Oluwakayode S. Oyedele<sup>2</sup> and Vershima D. Ashiekaa<sup>1</sup>

<sup>1</sup>Department of Chemical Engineering, Covenant University, Ota., Nigeria

<sup>2</sup>Department of Civil, Geo and Environmental Engineering, Technical University of Munich, Munich, Germany

#### Abstract:

#### Introduction:

Cardiovascular diseases are a known health threat with no respect for age. The need to understand the initiation and progress of the disease is expedient in proper diagnosis and management of the disease.

#### Objective:

The work is targeted at simulating the effect of elevated blood pressure on the initiation and development of plaque over time concerning wall shear stress, WSS and plaque wall stress, and PWS.

#### Methods:

Conditions such as blood velocity, pressure, and arterial wall conditions associated with blood flow in arteries, as well as patient-specific characterization related to these variables and conditions, were plugged into modified models in the COMSOL multiphysics software. The artery was modeled as an idealized 2-D carotid artery model.

#### Results:

Results showed that the WSS distribution with respect to changes with a blood pressure of 500 Pa gave the highest WSS value at the plaque neck and 1500 Pa gave the highest WSS value in the regions close to the plaque root. It was also observed that as the plaque size increased, the region experiencing severely high values for WSS also expanded.

#### Conclusion:

It can be recommended that blood pressure monitoring is necessary to curb the attendant cardiovascular diseases associated with high blood pressure.

**Keywords:** Wall shear stress, Cardiovascular disease, Newtonian fluid, Arterial plaque, Linear-elastic characteristics, CVDs.

#### Article History

Received: February 9, 2022

Revised: March 20, 2022

Accepted: March 25, 2022

## 1. INTRODUCTION

As of 2010, statistics showed that the probability of dying from a CVD is about 30%, indicating that fatalities from other diseases such as cancers are relatively insignificant [1]. He & Chen (2018) [2] showed that as of 2002, the World Health Organisation (WHO) had recognized cardiovascular diseases (CVDs) as an epidemic and concluded that efforts to combat the diseases had been a collateral failure. One of the reasons for

this failure was a lack of adequate knowledge of the disease and the implementation of scientific solutions. Unfortunately, the younger population is not an exception to the risk of this disease. Studies by Wang *et al.* (2017) [3] indicated that CVDs amongst the populace of ages < 45 years between 2010 and 2014 increased significantly. In the light of the current SARS-CoV-2 pandemic, CVDs are known to be the second-highest comorbidity that has led to deaths in recent times [4].

Atherosclerosis, caused by the clogging or hardening of the arteries induced by plaques, is a common cause of cerebrovascular and coronary diseases, which are the major

\* Address correspondence to this author at the Department of Chemical Engineering, Covenant University, Ota., Nigeria;  
E-mail: [edith.alagbe@covenantuniversity.edu.ng](mailto:edith.alagbe@covenantuniversity.edu.ng)

morbidities worldwide [5]. Over time, as research on the disease broadened, understanding of atherosclerosis has developed from the disease being caused by a plain accumulation of lipids within the innermost layer of the arterial wall [6] to being caused as a condition as an inflammatory response of the body resulting from lipid build-up which is usually initiated by the immune response of the body [7, 8]. When this occurs, there are two possible outcomes: the first is a hemorrhage into the plaque, and the second occurrence could be when blood clot forms on the plaque's surface (thrombus) [9]. This can occur in large and medium-sized arteries and could result in a crisis involving a stroke or heart attack, as the case may be [9].

The work of Vasava *et al.* (2012) [10] showed the effect of hypo- and hypertension by indicating that variations of blood pressure in a 3-D branched human aortic arch affect WSS distribution. The authors were able to show how hypertensive patients were at higher risk of atherogenesis due to low WSS distribution relative to hypotension. However, the work did not reveal how much these variations in blood pressure would affect the geometrical adaptation of the plaque in terms of the degree of stenosis. Liu & Tang (2010) [11] studied the three-dimensional mathematical model to investigate the geometrical adaptation of the atherosclerotic plaques in coronary arteries and study the influence of inlet flowrate, wall shear stress, and blood viscosity on the growth of atherosclerotic plaque. The authors implemented a linear plaque growth function that involved only the effect of WSS on the adaptation of the plaque over time and also assumed arterial wall rigidity. The work did not include the impact of principal stress of the plaque on the plaque geometry adaptation; also, the assumption of wall rigidity on the effect of plaque adaptation was neglected. Tian *et al.* (2013) [12] studied the impact of plaque geometry (in terms of height or width), blood pulsatile flow characteristics, Newtonian and Non-Newtonian blood flow characteristics on wall shear stress (WSS), wall shear stress gradient (WSSG) and wall-normal stress (WNS) distribution along a model 2-D blood vessel. The study was able to show the importance of plaque height on WSS distribution as against the width of the plaque, especially with Newtonian blood rheology. The area of interest the study downplayed was how vessel elasticity would affect these variables and their effects on plaque geometrical adaptation.

Alan *et al.* (2003) [1] studied the relationship between intima thickness, vessel distensibility age, and blood pressure in the coronary artery through non-invasive coronary angiography. They were able to show that in medium to large arteries, intima thickening (associated with plaque growth) affected the distensibility of the vessel considerably, so also they were able to show that blood pressure also affected vessel distensibility considerably. They realized that blood pressure (hypertension) was correlated highly with intima thickening. Their work highlighted the importance of deformability of the blood vessel on blood pressure and plaque development. (Veller *et al.*, 1993) [13] also observed that there was a positive relationship between systolic blood pressure in their non-invasive angiography studies of the common carotid artery, although they didn't tell by how much these variations can

affect intima thickening [14 - 16] also confirmed the importance of blood pressure on intima thickening. The FDA approved blood pressure as a biomarker [17], with systolic pressure seeming to be one of the most critical factors that affect intima thickening.

The implications of hemodynamic properties such as wall shear stress (WSS) on the pathogenesis of atherosclerosis have been studied extensively by works showing various connections between the two variables [11, 18, 19]. These works indicated a strong relationship between WSS and intima thickening, and a negative correlation was recorded in most cases. The work of Tang *et al.* (2008) [20] also gave insight as to how the normal stress on plaque (Plaque Wall Stress-PWS) also affects the rate of development of the plaque, and this was also referenced in the work of Dhawan *et al.*, (2010) [18]. These have given insight into the hemodynamic-based pathogenesis of the disease. However, not enough has been done by implementing these correlations to properly understand how much the plaque geometry adaptation would be affected by these variables and how fast this process can occur.

There is a need to model the possible variables and conditions such as blood velocity, pressure, and arterial wall conditions associated with blood flow in arteries, as well as patient-specific characterization associated with these variables and conditions. This would help explain how patients whose arteries conform to these characterizations would influence the initiation and progression of atherosclerosis.

The work aims at simulating the initiation and development of plaque over time, in relation to WSS and PWS, with a focus on the effect of elevated blood pressure on WSS and PWS and its overall impact on the plaque growth rate. The artery of focus here was an idealized 2-D carotid artery model.

## 2. METHODOLOGY

### 2.1. Vessel Model and Properties

The carotid artery model was a 2-D straight vessel with two domains; the lumen domain and the arterial wall domain. The wall of the artery was considered single-layered, homogenous, isotropic, and incompressible with linear-elastic characteristics [21]. The computational domain for the flow is described in Fig. (1). The dimensions used for the vessel model were adapted from studies [21 - 24] on the carotid artery with modifications, as indicated in Fig. (1). The vessel characteristics of the carotid artery model are indicated in Tables 1 and 2.

### 2.2. Blood Properties

Blood was assumed to be Newtonian, incompressible, and viscous when carrying out WSS studies in nature under the arterial conditions being studied [25]. Under the conditions studied, blood flow rheology was taken to be laminar due to Reynolds number values less than 2300; hence the consideration of turbulence was unnecessary. The blood parameters are assumed to be constant all through the flow process, and the absence of an underlying risk factor was also made.

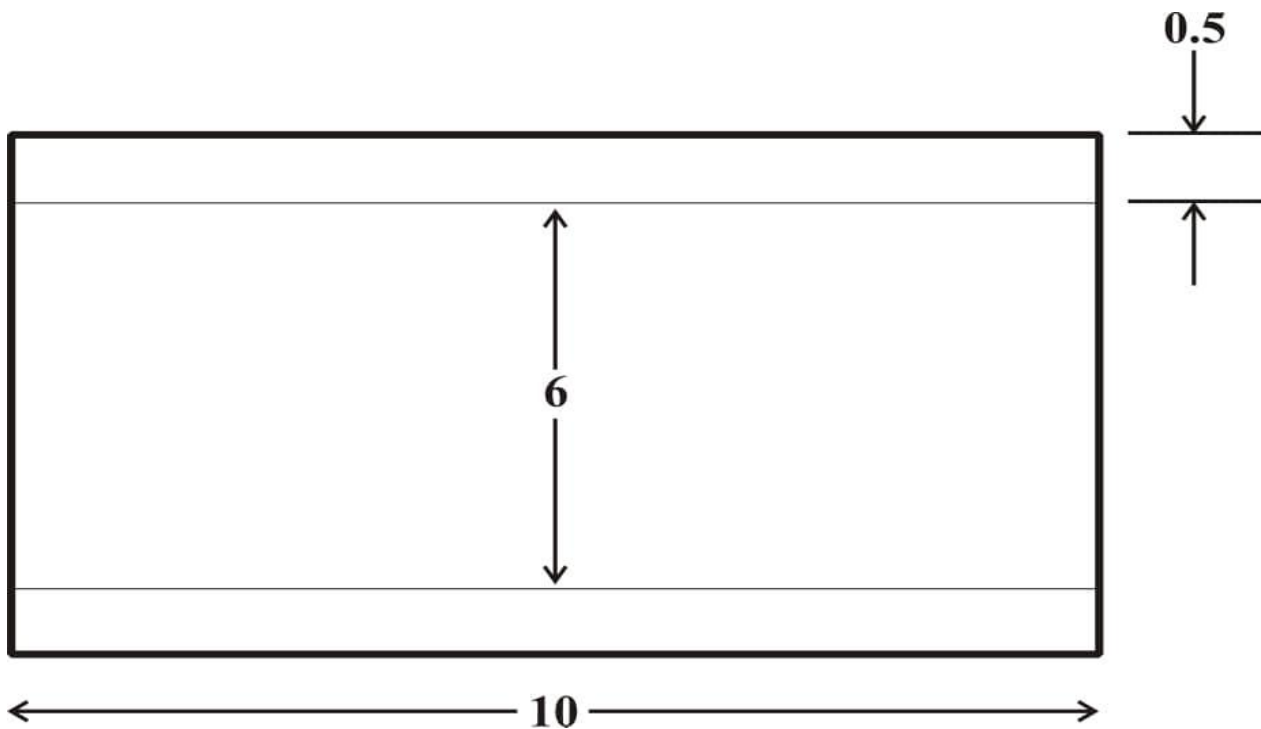


Fig. (1). Idealized carotid artery geometry constructed in COMSOL Multiphysics software (distances measured in mm).

Table 1. Carotid artery dimension and properties.

S/N	Parameter	Value	Source
1	Youngs Modulus	0.9 MPa	(Kumar <i>et al.</i> , 2020) [21]
2	Poisson Ratio	0.45	(Kumar <i>et al.</i> , 2020) [21]
3	Vessel length	10 mm	(Saxena <i>et al.</i> , 2019) [22]
4	Vessel Radius	6 mm	(Saxena <i>et al.</i> , 2019) [22]
5	Vessel Thickness	0.5 mm	(Kumar <i>et al.</i> , 2020; Stein, 2004) [21, 24]
6	Arterial wall density	1050 kg/m <sup>3</sup>	(Kumar <i>et al.</i> , 2020; Razavi <i>et al.</i> , 2011) [21, 23]

Table 2. Blood conditions.

S/N	Parameter	Value	Source
1	Rheology (Newtonian)	0.0035 Pa.s	Razavi <i>et al.</i> (2011) [23]
2	Blood density	1050 kg/m <sup>3</sup>	(Razavi <i>et al.</i> , 2011) [23]

2.3. Boundary Conditions

The assumption of the linear elastic arterial wall with parameters as shown in Table 1 was justified because arteries usually experience deformations ranging from 10 – 15% within the cardiac cycle of blood flow [26, 27]. This linear elastic model has also been computationally cost-effective, producing results that correlate satisfactorily with experimental data [28]. The common carotid artery is the section under investigation, and this section was constrained at the edges of the arterial wall to ensure the stability of the model during flow as well as a more realistic representation of the working of the artery (Kumar *et al.*, 2020). However, the remaining nodes were set to be free to ensure fluid-structure interaction between the

blood in the arterial lumen and the artery wall [20, 21, 29]. A fully developed Inlet velocity boundary condition was applied at the inlet of the artery, and a traction boundary pressure condition was applied at the outlet of the artery [11, 22, 30]. For simplicity and to save simulation time, it was assumed that the outlet pressure of the artery is the mean outlet pressure throughout the cardiac cycle and assumed to be constant throughout. The flow of blood at the artery wall was also assumed to experience a no-slip condition during the cardiac cycle. The velocity distribution along the vessel cross-section is defined by equations (1) to (3), where equation (4) is the zero-traction, zero-pressure boundary outlet condition.

$$u(r) = u_{max} \left[ 1 - \left( \frac{r}{R} \right)^2 \right] \tag{1}$$

$$v_{in} = u(r) \tag{2}$$

Where  $v_{in}$  represents the inlet velocity, and the artery's distribution is represented by the steady, fully developed velocity profile  $u(r)$ , where  $u_{max}$  is the maximum velocity, at the centre of the artery.

$$v_r = 0 \tag{3}$$

Where  $v_r$  is the velocity at the arterial wall boundary, which indicates a no-slip condition of zero-velocity condition.

$$P_{out} = P_i \tag{4}$$

Where  $P_{out}$  is the outlet boundary condition at the set pressure.

**2.4. Model Equation and Computational Set-up**

The flow in the arterial model was taken as a fluid-solid interaction (FSI) system consisting of the solid and liquid domain in connection interacting simultaneously. The Navier-Stokes equation for incompressible flow was used to model the blood flow in the artery (Eqs 5 and 6):

$$\rho_f (v \cdot \nabla v) - \nabla \cdot \sigma_f = 0 \tag{5}$$

$$\nabla \cdot v = 0 \text{ for the fluid domain} \tag{6}$$

Where  $\rho_f$  is the density of the blood  $v$  is the velocity field of the blood. Blood flow is described by the velocity and pressure field of the blood in the artery. Other external forces associated with gravity and movement of the human body are considered negligible hence they have been eliminated from the model.  $\sigma_f$  is the stress tensor and is represented by a function of pressure and velocity field of blood (Eq 7);

$$\sigma_f = -p_f I + 2\mu \varepsilon(v_f) \tag{7}$$

Where  $\mu$  is the blood viscosity,  $p_f$  is the Lagrange multiplier corresponding incompressibility constraint in equation 5,  $\varepsilon(v_f)$  is the strain-rate tensor (Eq 8):

$$\varepsilon(v_f) = \frac{1}{2} (\nabla v_f + (\nabla v_f)^T) \tag{8}$$

Where  $\tau_{ij}$  is the shear stress,  $\gamma_{ij}$  is the shear rate.

For the arterial wall structure, the model governing deformation in the structure is (Eq 9);

$$\rho_s ((\nabla v_s)v_s - g) - \nabla \cdot \sigma_s = 0 \text{ in } \Omega_w \text{ where} \tag{9}$$

Where  $s$  is the solid structure (arterial wall),  $\rho_s$  is the arterial density,  $g$  is the conglomerate of external body forces acting in the arterial wall, taken to be = 0,  $\sigma_s$  is the Cauchy stress tensor. With respect to a fixed reference state (Eq 10);

$$\rho_s \left( \frac{\partial^2 u_s}{\partial t^2} - g \right) - \nabla \cdot \sum_s = 0 \text{ in } \Omega_s \tag{10}$$

Where  $u_s$  is the vessel wall displacement  $\sum_s = J\sigma_s F^{-T}$  is the first Piola-Kirchoff tensor which represents the momentum equation (12). It is taken that the forces within the blood in the lumen also act on the lumen in an equal but opposite manner such that at the interface between the arterial wall blood in the lumen (Eq 11);

$$\sigma_f n = \sigma_s n v_f = v_s \text{ on } \Gamma_t^0 \tag{11}$$

Where  $n$  is the normal unit vector to the interface  $\Gamma_t$

**2.5. Mesh Independent Study**

Triangular meshes were used in discretizing the domain of the artery, as indicated in Fig. (2). The meshing was adapted to be more intricate around the boundaries and the wall/blood

interface to ensure that the interactions between both domains at the shear rates are accurately computed. The meshing was set to be fine because of optimal result accuracy and computational cost.

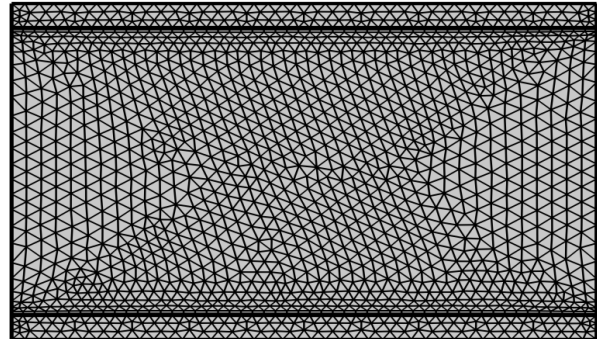


Fig. (2). Meshing of the Arterial domains (triangular meshing).

**2.6. Plaque Growth Modeling**

The plaque geometry was idealized, initiated, and made to progress at the centre length of the artery (5 mm), where the growth was extended from the arterial wall as the plaque progressed. The growth was taken to be an asymmetric blockage in the artery.

The plaque initiation and development model equation was based on the model developed by Tang *et al.* (2008) [20]. The model incorporates the negative correlation between the human carotid plaque progression (WTI) with plaque wall stress (PWS- $\sigma$ ) and flows shear stress (WSS- $\tau$ ) from in-vivo MRI-based studies. The uniqueness of the model is that, unlike earlier similar models that could not predict plaque initiation and growth at high shear stress (WSS) exposure, the authors extended the model further and discovered that there is still a relationship between plaque growth and the principal shear stress the plaque is exposed to (PWS). This model gave a new dimension to the initial model by incorporating a plaque wall stress (PWS) expression such that the linear function is expressed as:

Where  $\sigma$  is the principal shear stress represented as PWS in KPa,  $\tau$  is the flow shear stress represented as the WSS in Dyne/cm<sup>2</sup>, and WTI is the increase in plaque wall thickness, depicting the differential increase in plaque height relative to the initial plaque height in cm. This model predicts the height the plaque would have attained relative to the initial height every 304 days; hence it is assumed that 1 time /cycle of geometry update is 304 days (Eq 12);

$$WTI = 0.111 - 0.00103\sigma - 0.000663\tau \tag{12}$$

**2.7. Simulation Steps**

The protocol for implementing the model was adopted with modification from the work of Liu & Tang (2010) [11]. There are two major stages involved;

a) *Initiation Stage*: here, the plaque is initiated in the plaque-free artery. The protocol is such that;

i The initial arterial domain without atherosclerosis (plaque-free) is first considered, and the blood flow under the subjected conditions is solved.

ii The WSS and PWS values are obtained at the point of plaque initiation.

iii The WSS and PWS values are simultaneously inputted into the model to calculate the WTI.

iv Based on the WTI, the plaque is freshly initiated by adjusting the boundary of the arterial wall at the point of stenosis.

b *Progression Stage:* here, the plaque progresses relative to the memory of the initial plaque condition.

i After the arterial wall boundary has been adjusted to suit the plaque initiation, The fluid-structure interaction (FSI) model is solved again to obtain the WSS and PWS.

ii The PWS and WSS values were simultaneously inputted into the model to calculate the WTI.

iii The new height of the plaque was adjusted by adding the new WTI value.

iv The sequence was repeated until the target time of exposure (after a couple of years of geometry update) was reached.

After each geometry update, the plaque height is increased. Hence stenosis becomes severe. The degree of stenosis/stenosis severity measures the amount of the arterial lumen that has been occluded (in terms of luminal diameter) by the plaque. It restricts blood flow in the axial direction. Here, stenosis measures the degree of the progression of atherosclerosis in the carotid artery. This can be calculated as shown in Eq (13):

$$\% \text{ Stenosis} = \frac{\text{height of plaque}}{\text{Overall lumen diameter}} * 100 \quad (13)$$

### 3. RESULTS AND DISCUSSION

#### 3.1. Effect of Blood Pressure Variation on WSS and PWS

Figs. (3 and 4) show the WSS and PWS distribution along the vessel wall with a plaque after the initiation of the plaque at 17% stenosis at an outlet pressure range from 500 Pa to 1500 Pa, which is meant to mimic the effect of variation of WSS and PWS with blood pressure build-up. It can be observed that in all cases of outlet pressure, the highest WSS and PWS still characteristically occurred at the stenosis neck. Moreover, the root of the plaque characteristically experienced the least WSS and PWS. In a comparison of this distribution for the various outlet pressures considered, it can be seen that the least outlet pressure of 500 Pa gave the highest WSS and PWS at the neck region of the plaque, with the 1500 Pa outlet pressure having the least; however, for regions around the root of the plaque, the reverse is the case. The insight that can be drawn here is that the root of the plaque is the region that is the most structurally vulnerable to rupture. High blood pressure causes high WSS and PWS in these regions, which could be the major reason patients with high blood pressure suffer a higher risk of stroke due to a higher risk of plaque rupture associated with high WSS and PWS values. From Fig. (4), it can be observed that regions close to the neck of the plaque tend to experience compressive stress against regions away or around the root of the plaque, which undergoes tensile stresses.

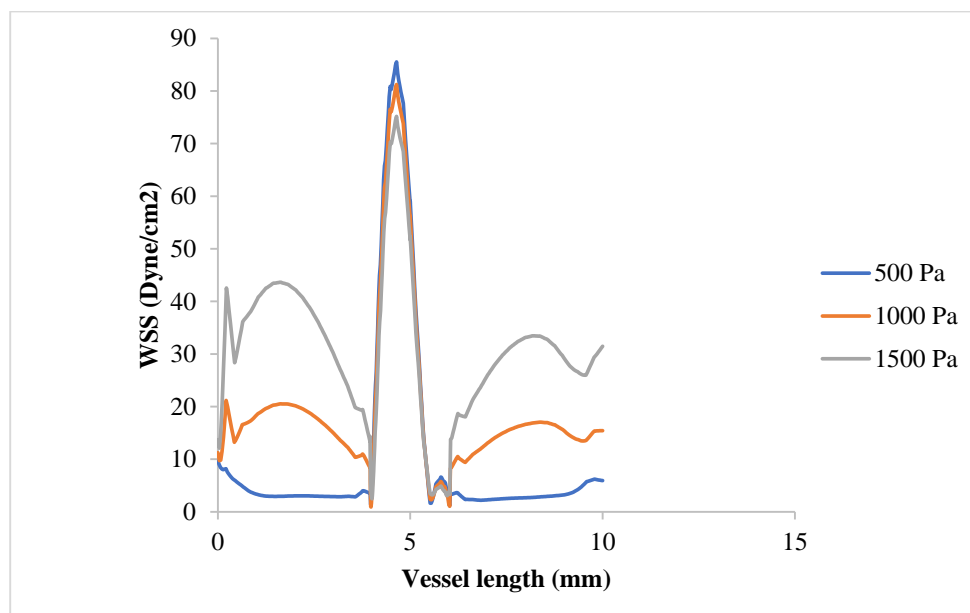


Fig. (3). WSS distribution along the arterial length at initiation stage (17.3%) at different outlet pressures at 30 cm/s inlet velocity.

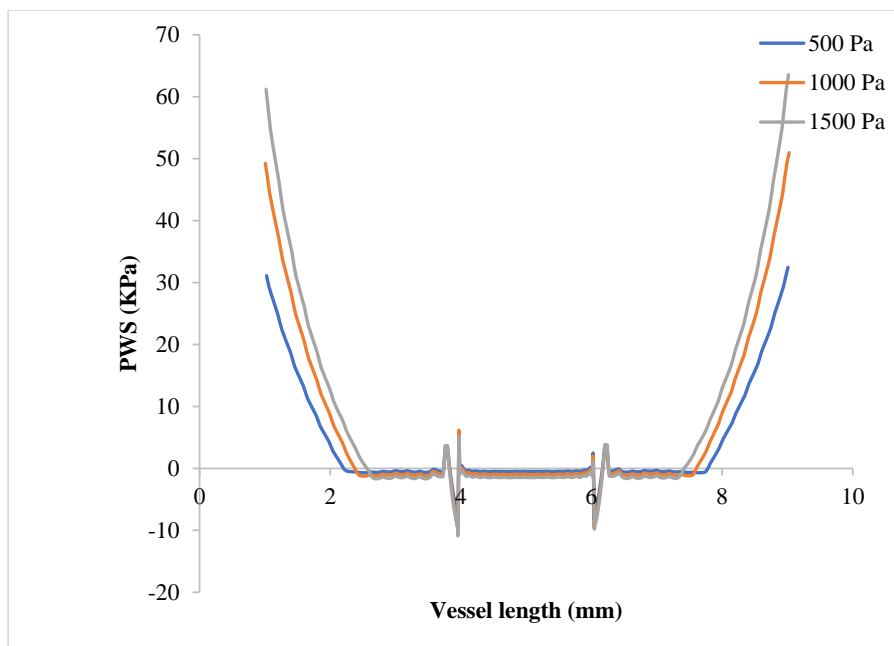


Fig. (4). PWS distribution along the arterial length at the initiation stage (17.3%) at a different outlet pressure.

Fig. (4) shows that the WSS has risen to values around twice what it was where the plaque had grown to 17.3% of the vessel diameter. It can be observed that the WSS distribution with respect to changes in blood pressure still follows that 500 Pa gave the highest WSS value at the plaque neck and 1500 Pa gave the highest WSS value at the regions close to the plaque root. It can also be observed that as the plaque size increased, the region experiencing severely high values for WSS also expanded. From Figs. (5 and 6), the WSS and PWS distribution was computed after the plaque had grown to a point the blood vessel lumen diameter had been blocked by half its initial value. Alternatively, comparing Fig. (4) with Fig. (6), there is a stress shift, more from the tensile stress seen in the 17.3% stenosis to more compressive stress as the plaque grew to 50% stenosis, compressional stresses.

From Fig. (7), as the plaque grew to 80% stenosis, maximum WSS has shot up to 7 times the initial value at 17.3% stenosis. The wall of the plaque experienced tremendous WSS, hence indicating that the growth in this region is doubtful. It can also be observed that in regions away from the neck of the stenosis, especially around the arterial wall, pressure variation did not lead to any substantial change in WSS at those regions. Fig. (8) shows a tremendous drop in PWS by about 13 times its initial value when compared to that of the 50% stenosis, so also, no tensile stresses were experienced on the plaque and regions of the arterial wall connected to the plaque. This is because the stresses have been transferred to the inner arterial wall opposite where the plaque is located due to the asymmetrical geometry of the plaque in the vessel.

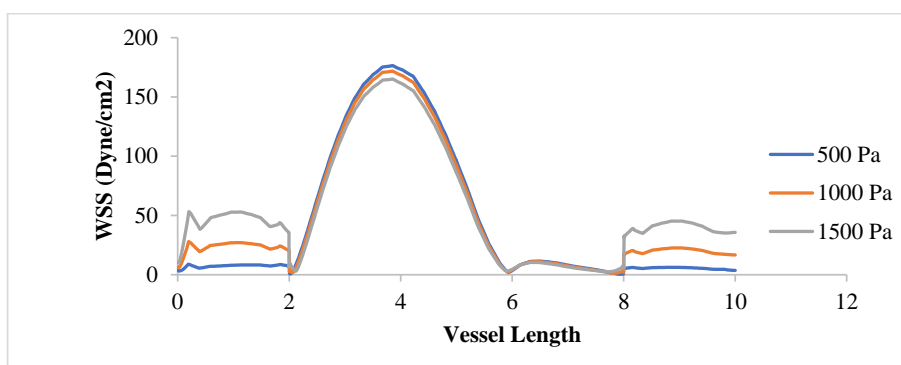


Fig. (5). WSS distribution along the arterial length at 50% stenosis stage at different outlet pressures at 30 cm/s inlet velocity.

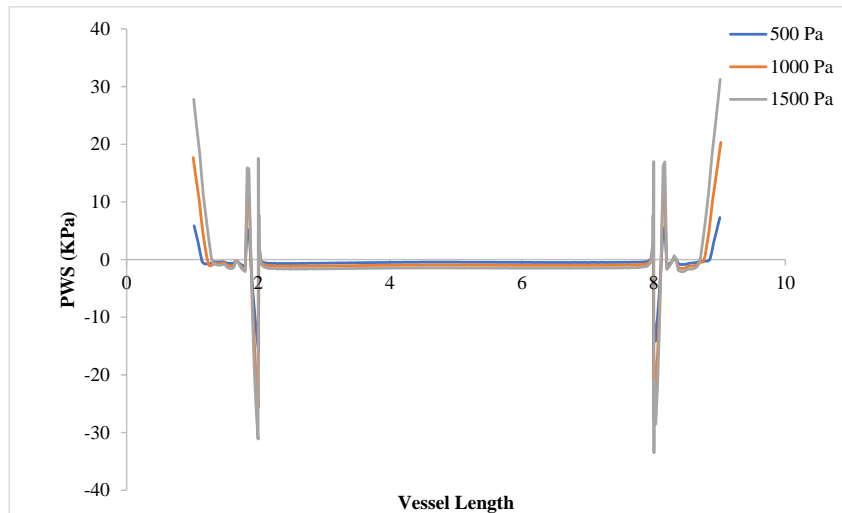


Fig. (6). PWS distribution along the arterial length at 50% stenosis stage at different outlet pressures.

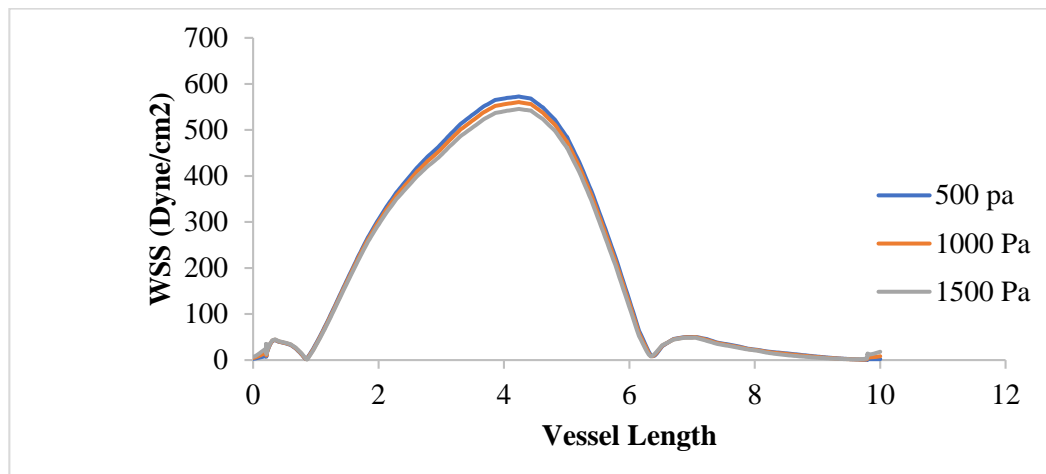


Fig. (7). WSS distribution along the arterial length at 80% stenosis stage at different outlet pressures at 30 cm/s inlet velocity.

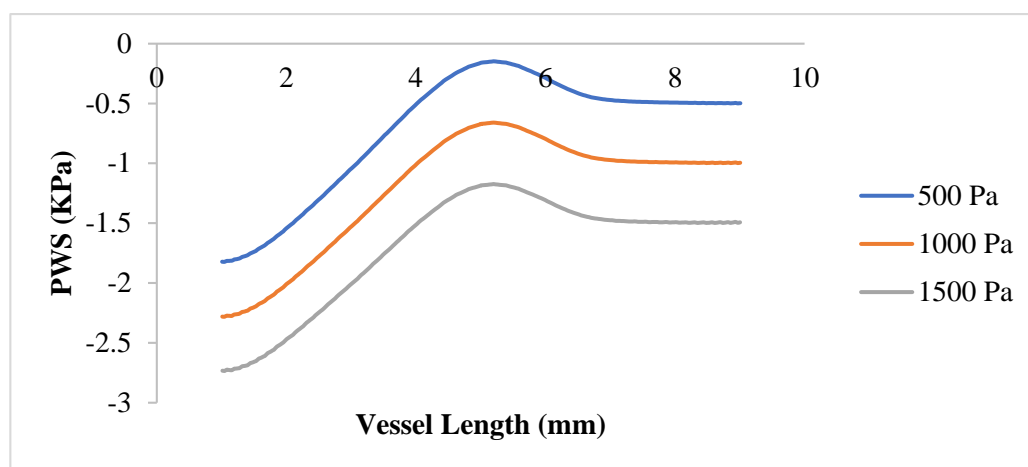


Fig. (8). PWS distribution along the arterial length at 80% stenosis stage at different outlet pressures.

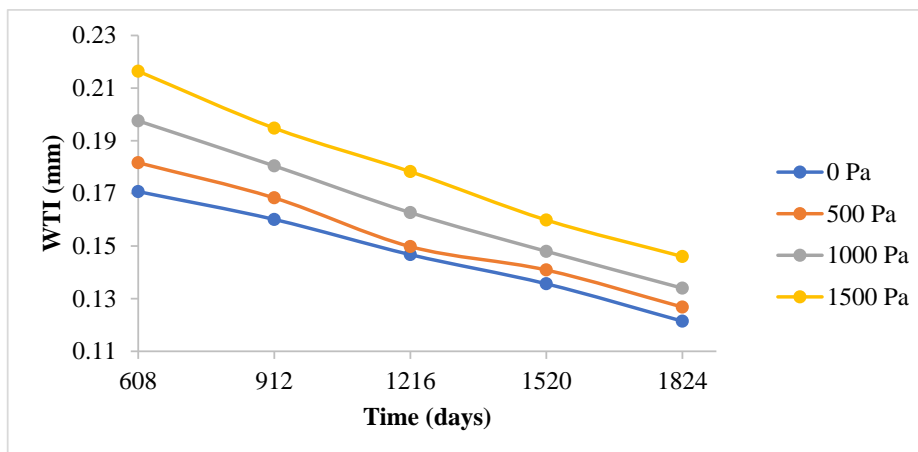


Fig. (9). Differential increase in plaque height every 304 days for 5 years.

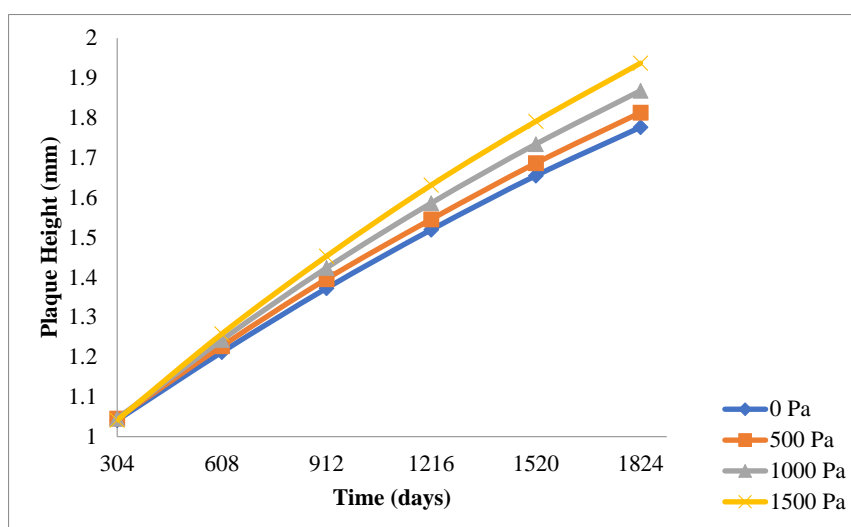


Fig. (10). Overall plaque height for 5 years.

### 3.2. Plaque Initiation and Development Associated with Blood Pressure

A general reduction in the plaque growth rate as time elapsed is also observed here in Fig. (9 and 10). The essence of this study is to give a holistic insight into how variations in blood pressure would affect the overall plaque height after some time, as well as the rate of plaque growth. Fig. (9) indicates that all through the period studied, the carotid artery experiencing the highest outlet pressure had the highest rate of plaque progression all through. The least outlet pressure had the least rate of plaque growth all through the period studied. This indicates that higher blood pressure tends to give WSS and PWS values that accelerate the rate of development of the plaque in the carotid artery.

Fig. (10) shows the cumulative effect the development rate of the plaque has on the overall plaque height at different outlet pressures. It can be observed that the highest pressure of 1500 Pa gave the highest overall plaque height leading to stenosis of 32.2%, while the least pressure of 0 Pa gave the least overall plaque height leading to vessel stenosis of about 2.95%.

Although these variations may not be significant compared to the effect that the blood velocity variations had on the overall plaque height, this gives insight as to how blood pressure too can contribute to the development of a plaque in the carotid artery.

### CONCLUSION

It can be concluded that an increase in blood pressure operates such that the WSS and PWS cause a resultant increase in the rate of plaque development and the overall plaque height. As the stenosis increases, the PWS becomes more compressional on the plaque. The results explicitly show the consequence of elevated blood pressure in the carotid artery on the rate of plaque growth and risk of rupture. Blood pressure regulation plays a significant role in the initiation and development of atherosclerosis in the carotid artery and the resultant risk of stroke. It is, therefore, recommended that adequate monitoring of blood pressure be carried out regularly and controlled within limits to prevent the occurrence of atherosclerosis.

## CONSENT FOR PUBLICATION

Not applicable.

## AVAILABILITY OF DATA AND MATERIALS

Not applicable.

## FUNDING

The Team appreciates the financial support of Covenant University in publishing this manuscript and the collaborative support of the Technical University of Munich, Germany.

## CONFLICT OF INTEREST

The authors declare no conflict of interest, financial or otherwise.

## ACKNOWLEDGEMENTS

The team appreciates the financial support of Covenant University in publishing this manuscript and the collaborative support of the Technical University of Munich, Germany.

## REFERENCES

- [1] S. Alan, M.S. Ulgen, O. Ozturk, B. Alan, L. Ozdemir, and N. Toprak, "Relation between coronary artery disease, risk factors and intima-media thickness of carotid artery, arterial distensibility, and stiffness index", *Angiology*, vol. 54, no. 3, pp. 261-267, 2003. [http://dx.doi.org/10.1177/000331970305400301] [PMID: 12785018]
- [2] Z. He, and Z-Y. Chen, "The origin of trimethylamine-N-oxide (TMAO) and its role in the development of atherosclerosis", *J. Food Bioact.*, vol. 2, no. 1, pp. 68-75, 2018. [http://dx.doi.org/10.31665/JFB.2018.2138]
- [3] X. Wang, M. Gao, S. Zhou, J. Wang, F. Liu, F. Tian, J. Jin, Q. Ma, X. Xue, J. Liu, Y. Liu, and Y. Chen, "Trend in young coronary artery disease in China from 2010 to 2014: a retrospective study of young patients  $\leq 45$ ", *BMC Cardiovasc. Disord.*, vol. 17, no. 1, p. 18, 2017. [http://dx.doi.org/10.1186/s12872-016-0458-1] [PMID: 28061763]
- [4] G. Grasselli, A. Zangrillo, A. Zanella, M. Antonelli, L. Cabrini, A. Castelli, D. Cereda, A. Coluccello, G. Foti, R. Fumagalli, G. Iotti, N. Latronico, L. Lorini, S. Merler, G. Natalini, A. Piatti, M.V. Ranieri, A.M. Scandroglio, E. Storti, M. Cecconi, A. Pesenti, E. Agosteo, V. Alaimo, G. Albano, A. Albertin, A. Alborghetti, G. Aldegheri, B. Antonini, E. Barbara, N. Belgioirno, M. Belliato, A. Benini, E. Beretta, L. Bianciardi, S. Bonazzi, M. Borelli, E. Boselli, N. Bronzini, C. Capra, L. Carnevale, G. Casella, G. Castelli, E. Catena, S. Cattaneo, D. Chiumello, S. Cirri, G. Citerio, S. Colombo, D. Coppini, A. Corona, P. Cortellazzi, E. Costantini, R.D. Covoello, G. De Filippi, M. Dei Poli, F. Della Mura, G. Evasi, R. Fernandez-Olmos, A. Forastieri Molinari, M. Galletti, G. Gallioli, M. Gemma, P. Gnesin, L. Grazioli, S. Greco, P. Gritti, P. Grosso, L. Guatterri, D. Guzzon, F. Harizay, R. Keim, G. Landoni, T. Langer, A. Lombardo, A. Malara, E. Malpetti, F. Marino, G. Marino, M.G. Mazzoni, G. Merli, A. Micucci, F. Mojoli, S. Muttini, A. Nailescu, M. Panigada, P. Perazzo, G.B. Perego, N. Petrucci, A. Pezzi, A. Protti, D. Radrizzani, M. Raimondi, M. Ranucci, F. Rasulo, M. Riccio, R. Rona, C. Roscitano, P. Ruggeri, A. Sala, G. Sala, L. Salvi, P. Sebastiano, P. Severgnini, I. Sforzini, F.D. Sigurtà, M. Subert, P. Tagliabue, C. Troiano, R. Valsecchi, U. Viola, G. Vitale, M. Zambon, and E. Zoia, "Baseline Characteristics and Outcomes of 1591 Patients Infected With SARS-CoV-2 Admitted to ICUs of the Lombardy Region, Italy", *JAMA*, vol. 323, no. 16, pp. 1574-1581, 2020. [http://dx.doi.org/10.1001/jama.2020.5394] [PMID: 32250385]
- [5] Rosamond, "Erratum: Heart disease and stroke statistics-2008 update: A report from the American Heart Association statistics committee and stroke statistics subcommittee (Circulation (2008) 117 (e25-e146))", In: *Circulation*, 2010. [http://dx.doi.org/10.1161/CIR.0b013e3181e65b27]
- [6] P. Libby, A.H. Lichtman, and G.K. Hansson, "Immune effector mechanisms implicated in atherosclerosis: From mice to humans", In: *Immunity*, vol. 38, 2013, no. 6, pp. 1092-1104. [http://dx.doi.org/10.1016/j.immuni.2013.06.009]
- [7] I. Joris, and G. Majno, "Atherosclerosis and inflammation", *Adv. Exp. Med. Biol.*, vol. 104, no. 6, pp. 227-243, 1978. [http://dx.doi.org/10.1007/978-1-4684-7787-0\_10] [PMID: 717133]
- [8] C. Weber, and H. Noels, "Atherosclerosis: Current pathogenesis and therapeutic options", In: *Nature Medicine*, vol. 17, 2011, no. 11, pp. 1410-1422. [http://dx.doi.org/10.1038/nm.2538]
- [9] R.N. Pralhad, and D.H. Schultz, "Modeling of arterial stenosis and its applications to blood diseases", *Math. Biosci.*, vol. 190, no. 2, pp. 203-220, 2004. [http://dx.doi.org/10.1016/j.mbs.2004.01.009] [PMID: 15234617]
- [10] P. Vasava, P. Jalali, M. Dabagh, and P.J. Kolar, "Finite element modelling of pulsatile blood flow in idealized model of human aortic arch: study of hypotension and hypertension", *Comput. Math. Methods Med.*, vol. 2012, no. 10, p. 861837, 2012. [http://dx.doi.org/10.1155/2012/861837] [PMID: 22400055]
- [11] B. Liu, and D. Tang, "Computer simulations of atherosclerotic plaque growth in coronary arteries", *Mol. Cell. Biomech.*, vol. 7, no. 4, pp. 193-202, 2010. [http://dx.doi.org/10.3970/mcb.2010.007.193] [PMID: 21141673]
- [12] F.B. Tian, L. Zhu, P.W. Fok, and X.Y. Lu, "Simulation of a pulsatile non-Newtonian flow past a stenosed 2D artery with atherosclerosis", *Comput. Biol. Med.*, vol. 43, no. 9, pp. 1098-1113, 2013. [http://dx.doi.org/10.1016/j.combiomed.2013.05.023] [PMID: 23930803]
- [13] M.G. Veller, C.M. Fisher, A.N. Nicolaides, S. Renton, G. Geroulakos, N.J. Stafford, A. Sarker, G. Szendro, and G. Belcaro, "Measurement of the ultrasonic intima-media complex thickness in normal subjects", *J. Vasc. Surg.*, vol. 17, no. 4, pp. 719-725, 1993. [http://dx.doi.org/10.1016/0741-5214(93)90116-4] [PMID: 8464091]
- [14] O. Azeta, A.O. Ayeni, O. Agboola, and F.B. Elehinafe, "A review on the sustainable energy generation from the pyrolysis of coconut biomass", *Scientific African*, vol. 2021, no. 13, p. e00909, 2021. [http://dx.doi.org/10.1016/j.sciaf.2021.e00909]
- [15] K. Al-Shali, A.A. House, A.J.G. Hanley, H.M.R. Khan, S.B. Harris, M. Mamakeesick, B. Zinman, A. Fenster, J.D. Spence, and R.A. Hegele, "Differences between carotid wall morphological phenotypes measured by ultrasound in one, two and three dimensions", *Atherosclerosis*, vol. 178, no. 2, pp. 319-325, 2005. [http://dx.doi.org/10.1016/j.atherosclerosis.2004.08.016] [PMID: 15694940]
- [16] C. Lemne, T. Jogestrand, and U. de Faire, "Carotid intima-media thickness and plaque in borderline hypertension", *Stroke*, vol. 26, no. 1, pp. 34-39, 1995. [http://dx.doi.org/10.1161/01.STR.26.1.34] [PMID: 7839394]
- [17] P.J. Touboul, M.G. Hennerici, S. Meairs, H. Adams, P. Amarenco, N. Bornstein, L. Csiba, M. Desvarieux, S. Ebrahim, M. Fatar, R. Hernandez Hernandez, M. Jaff, S. Kownator, P. Prati, T. Rundek, M. Sitzer, U. Schminke, J.C. Tardif, A. Taylor, E. Vicaut, K.S. Woo, F. Zannad, and M. Zureik, "Mannheim carotid intima-media thickness consensus (2004-2006). An update on behalf of the Advisory Board of the 3rd and 4th Watching the Risk Symposium, 13th and 15th European Stroke Conferences, Mannheim, Germany, 2004, and Brussels, Belgium, 2006", *Cerebrovasc. Dis.*, vol. 23, no. 1, pp. 75-80, 2007. [http://dx.doi.org/10.1159/000097034] [PMID: 17108679]
- [18] S.S. Dhawan, R.P.A. Nanjundappa, J.R. Branch, W.R. Taylor, A.A. Quyyumi, H. Jo, M.C. McDaniel, J. Suo, D. Giddens, and H. Samady, "Shear stress and plaque development", In: *Expert Review of Cardiovascular Therapy*, vol. 8, 2010, no. 4, pp. 545-556. [http://dx.doi.org/10.1586/erc.10.28]
- [19] B. Zhang, J. Gu, M. Qian, L. Niu, H. Zhou, and D. Ghista, "Correlation between quantitative analysis of wall shear stress and intima-media thickness in atherosclerosis development in carotid arteries", *Biomed. Eng. Online*, vol. 16, no. 1, p. 137, 2017. [http://dx.doi.org/10.1186/s12938-017-0425-9] [PMID: 29208019]
- [20] D. Tang, C. Yang, S. Mondal, F. Liu, G. Canton, T.S. Hatsukami, and C. Yuan, "A negative correlation between human carotid atherosclerotic plaque progression and plaque wall stress: in vivo MRI-based 2D/3D FSI models", *J. Biomech.*, vol. 41, no. 4, pp. 727-736, 2008. [http://dx.doi.org/10.1016/j.jbiomech.2007.11.026] [PMID: 18191138]
- [21] N. Kumar, S.M.A. Khader, R. Pai, S.H. Khan, and P.A. Kyriacou, "Fluid structure interaction study of stenosed carotid artery considering the effects of blood pressure", *Int. J. Eng. Sci.*, vol. 154, no. 1, p. 12, 2020.

- [http://dx.doi.org/10.1016/j.ijengsci.2020.103341]
- [22] A. Saxena, E.Y.K. Ng, M. Mathur, C. Manchanda, and N.A. Jajal, "Effect of carotid artery stenosis on neck skin tissue heat transfer", *Int. J. Therm. Sci.*, vol. 145, no. 1, pp. 278-300, 2019. [http://dx.doi.org/10.1016/j.ijthermalsci.2019.106010]
- [23] A. Razavi, E. Shirani, and M.R. Sadeghi, "Numerical simulation of blood pulsatile flow in a stenosed carotid artery using different rheological models", *J. Biomech.*, vol. 44, no. 11, pp. 2021-2030, 2011. [http://dx.doi.org/10.1016/j.jbiomech.2011.04.023] [PMID: 21696742]
- [24] J.H. Stein, "Carotid intima-media thickness and vascular age: you are only as old as your arteries look", *J. Am. Soc. Echocardiogr.*, vol. 17, no. 6, pp. 686-689, 2004. [http://dx.doi.org/10.1016/j.echo.2004.02.021] [PMID: 15163946]
- [25] B.M. Johnston, P.R. Johnston, S. Corney, and D. Kilpatrick, "Non-Newtonian blood flow in human right coronary arteries: transient simulations", *J. Biomech.*, vol. 39, no. 6, pp. 1116-1128, 2006. [http://dx.doi.org/10.1016/j.jbiomech.2005.01.034] [PMID: 16549100]
- [26] M-A. Etim, S. Academe, P. Emenike, and D. Omole, "Application of multi-criteria decision approach in the assessment of medical waste management systems in Nigeria", *Sustainability (Basel)*, vol. 13, no. 19, p. 10914, 2021. [http://dx.doi.org/10.3390/su131910914]
- [27] S.W. Cho, S.W. Kim, M.H. Sung, K.C. Rou, and H.S. Ryou, "Fluid-structure interaction analysis on the effects of vessel material properties on blood flow characteristics in stenosed arteries under axial rotation", *Korea-Australia Rheol. J.*, vol. 23, no. 1, pp. 7-16, 2011. [http://dx.doi.org/10.1007/s13367-011-0002-x]
- [28] R. Torii, M. Oshima, T. Kobayashi, K. Takagi, and T.E. Tezduyar, "Fluid-structure interaction modeling of blood flow and cerebral aneurysm: Significance of artery and aneurysm shapes", *Comput. Methods Appl. Mech. Eng.*, vol. 198, no. 45-46, pp. 3613-3621, 2009. [http://dx.doi.org/10.1016/j.cma.2008.08.020]
- [29] E. Misiulis, A. Džiugys, R. Navakas, and N. Striūgas, "A fluid-structure interaction model of the internal carotid and ophthalmic arteries for the noninvasive intracranial pressure measurement method", *Comput. Biol. Med.*, vol. 84, no. 1, pp. 79-88, 2017. [http://dx.doi.org/10.1016/j.combiomed.2017.03.014] [PMID: 28346876]
- [30] A. Valencia, and M. Villanueva, "Unsteady flow and mass transfer in models of stenotic arteries considering fluid-structure interaction", *Int. Commun. Heat Mass Transf.*, vol. 33, no. 8, pp. 966-975, 2006. [http://dx.doi.org/10.1016/j.icheatmasstransfer.2006.05.006]

© 2022 Alagbe et al.

This is an open access article distributed under the terms of the Creative Commons Attribution 4.0 International Public License (CC-BY 4.0), a copy of which is available at: <https://creativecommons.org/licenses/by/4.0/legalcode>. This license permits unrestricted use, distribution, and reproduction in any medium, provided the original author and source are credited.